ELSEVIER

Journal of Alloys and Compounds 224 (1995) 121–126

Journal of ALLOYS AND COMPOUNDS

Hydrogen absorbing-desorbing properties and crystal structure of the Zr–Ti–Ni–Mn–V AB_2 Laves phase alloys

M. Yoshida [a], E. Akiba [b]

[a] *Hitachi Chemical Co., Ltd. Tsukuba Research Laboratory, 48 Wadai, Tsukuba city, Ibaraki 300-42, Japan*

[b] *National Institute of Materials and Chemical Research, 1-1 Higashi, Tsukuba city, Ibaraki 305, Japan*

Received 22 July 1994; in final form 7 December 1994

Abstract

The effect of the substitution of Ti for the Zr (A) site and V for the Mn (B) site of $ZrNi_{1.3}Mn_{0.7}$ on the hydrogen absorbing-desorbing properties and crystal structure was studied by measuring pressure-composition (PC) isotherms at 313 K and by X-ray powder diffraction measurements. There exist three phases, the C14 and C15 Laves phases and the BCC solid solution phase in twelve alloys studied ($Zr_{1-x}Ti_xNi_{1.3}Mn_{0.7-y}V_y$, $x=0$, 0.1, 0.2, 0.5; $y=0$, 0.1, 0.2, 0.4, 0.7). The lattice parameter of the alloys containing the C15 Laves phase decreased as Ti (A-site) content was increased; contrarily it increased as V (B-site) content was increased. The PC isotherms of the alloys with the C15 Laves phase indicated that the equilibrium plateau pressure increased with increasing Ti content, but decreased with increasing V content. The hysteresis observed in the PC isotherm was reduced by substitution of Ti and V in the A and B sites, respectively.

Keywords: Laves phase; Alloys; Hydrogen; Crystal structure; Substitution

1. Introduction

Hydrogen absorbing alloys are expected to be a promising material for secondary batteries [1]. The use of $LaNi_5$-related alloys with $CaCu_5$-type structure is well known for practical electrodes of nickel–hydrogen rechargeable batteries [2]. Recently, Zr-based AB_2 Laves phase alloys ($ZrMn_2$ and ZrV_2) have attracted attention as second generation materials for electrodes because of their larger hydrogen absorbing-desorbing capacity in comparison with $LaNi_5$ [3]. AB_2 Laves phases are categorized into three types: $MgZn_2$-type structures (so called C14 phase), $MgCu_2$-type structures (C15 phase) and $MgNi_2$-type structures (C36 phase) [4]. Appearance of a particular Laves phase is determined by atomic size and electron–atom ratio [4]. It is important to pay attention not only to the size factor but also to the electronic factor in order to study the Laves phase alloys. Practical Laves phase alloys for hydrogen storage have the C14 or C15 phase. $ZrMn_2$ and ZrV_2 are representatives of the C14 and C15 phases, respectively [5,6].

Substitution is one of the most widely used methods to control the physical properties of the hydrogen absorbing alloys. It was particularly important to investigate the effect of substitution of the replacing elements on the hydrogen absorbing properties for design of the alloy. There have been several studies to clarify the effects of substitution for the Mn (B) site of $ZrMn_2$. Yonezu et al. [7] reported that the slope of the plateau in the isotherm was decreased by substituting Co for the Mn (B) site of $ZrMn_2$, and the hysteresis decreased by substituting Al for the Mn (B) site. Fujitani et al. [1] found a linear relationship between the logarithm of the equilibrium plateau pressure ($\ln P_{plateau}$) and the unit cell volume in $ZrMn_{2-x}M_x$ (M = V, Fe, Co and Ni). One of the present authors studied the crystal structure of $ZrMn_{2-x}M_x$ (M = V, Fe, Co, Ni and Al) and their deuterides using neutron diffraction in order to determine the position of the M metals and hydrogen [8]. The crystal structure of $ZrMn_2$ deuteride is reported to have two kinds of Mn sites [9]. All the replacing elements (V, Fe, Co, Ni and Al) were found to randomly occupy the two Mn sites. On the other hand, Pourarian et al. [10] studied the change in the lattice parameters and the hydrogen equilibrium pressure by replacing Zr (A) site of $ZrMn_2$ with Ti. They found that as the amount of the replacing element increased, the lattice parameter decreased and the equilibrium pressure increased. However, there was no structural report concerning the site occupancy of Ti on $Zr_{1-x}Ti_xMn_2$ alloys.

SSDI 0925-8388(95)01518-3

So far, researchers have studied the effect of the substitution on either the A or B site (so called mono-substitution) of the AB_2 alloys. However, the mutual effects of substitution of both A and B sites on the properties of the hydrogen-absorbing alloy, for example the equilibrium plateau pressure, hydrogen absorbing capacity and hysteresis, were not studied.

The purpose of this work was to study the effect of simultaneous substitution of Ti in the Zr (A) site and of V in the Mn (B) site of $ZrNi_{1.3}Mn_{0.7}$ on hydrogen absorbing-desorbing properties. We also investigated the relationship between these properties and lattice parameters. $ZrMn_2$ was the most suitable standard material for the study concerning the effect of the substitution. Some fundamental research was already done [5,10,11]. From this investigation the hydride of $ZrMn_2$ appeared very stable [10]. $ZrMn_2$ did not reversibly react with hydrogen around room temperature. We needed the substitution of another element in order to increase the equilibrium plateau pressure of $ZrMn_2$. It was known that by the substitution of Ni in the Mn site [11] the hydrogen equilibrium plateau pressure rose and the slope of the plateau reduced. Then, we considered that $ZrNi_{1.3}Mn_{0.7}$ was one of the suitable compositions for reversible reaction between hydrogen and alloys at ambient temperature. Ti and V were adopted as replacing elements on the A and B sites, respectively, because they were the typical constituent elements of the Laves phase, such as $TiCr_2$ [12] and ZrV_2 [6].

2. Experimental

The $Zr_{1-x}Ti_xNi_{1.3}Mn_{0.7-y}V_y$ ($x=0$, 0.1, 0.2, 0.5; $y=0$, 0.1 0.2, 0.4, 0.7) alloys were prepared by arc melting from 99.9% pure metals in argon atmosphere. The homogeneous samples were obtained by turning out and re-melting the alloy four times. It was very important for synthesis of homogeneous samples that the button on the water-cooling plate in the arc melt furnace was turned out as quickly as possible and re-melted before it cooled. When we prepared the intermetallic compounds that were usually brittle, they were very easily broken during the cooling process.

X-ray powder diffraction data of all the alloys were measured in a RIGAKU RAD-A diffractometer with CuKα radiation. The structure parameters were refined from the diffraction data with a Rietveld refinement program RIETAN-92 [13].

The pressure-composition (PC) isotherms at 313 K were measured by a conventional constant volume apparatus [14]. Before PC isotherm measurements, all the alloys were activated by evacuating at 473 K for 3 h and by introducing hydrogen up to 5 MPa at room temperature for 3 h. This treatment was repeated three times.

The argon-filled glove box was used to handle the activated samples .

3. Result and discussion

3.1. Phase stability and lattice parameters

C14, C15 phase and a small amount of the BCC phase [15] were found in the $Zr_{1-x}Ti_xNi_{1.3}Mn_{0.7-y}V_y$ ($x=0$, 0.1, 0.2, 0.5; $y=0$, 0.1, 0.2, 0.4, 0.7) alloys by X-ray diffraction analysis. All the samples contained a small amount of the minor BCC phase [15]. For X-ray Rietveld analysis of all the alloys, we considered the model with the following assumptions: (1) Ti goes into the Zr (A) site. (2) V and Ni randomly occupy the Mn (B) site as found in $Zr(Mn_{1-x}M_x)_2$ (M= V, Fe, Ni, Co and Al) [8]. (3) The BCC phase is a solid solution of all the elements and contains a W-type structure assigned to the $Im\bar{3}m$ space group. (4) Both C14 and C15 phases in an alloy have the same composition. Fig. 1 shows the result of Rietveld refinement for $Zr_{0.5}Ti_{0.5}Ni_{1.3}Mn_{0.5}V_{0.2}$ containing three phases (C14 phase: $R_I=4.9\%$, $R_F=4.1\%$, C15 phase: $R_I=3.7\%$, $R_F=3.2\%$, BCC phase: $R_I=2.2\%$, $R_F=2.7\%$, S (R_{wp}/R_e)=1.9). All the measured profiles of the prepared samples fitted well to those derived from the model adopted. The obtained R factors were in the range of R_I, $R_F<10\%$ and$S(R_{wp}/R_e)<3$.

The phase abundance was estimated using structure parameters obtained from Rietveld analysis. The phase abundance by weight (w_i) of each phase was related to the scale factor by the following equation [15, 16]:

$$w_i = \frac{(S_i \cdot D_i \cdot V_i^2)}{\sum_j (S_j \cdot D_j \cdot V_j^2)} \quad (1)$$

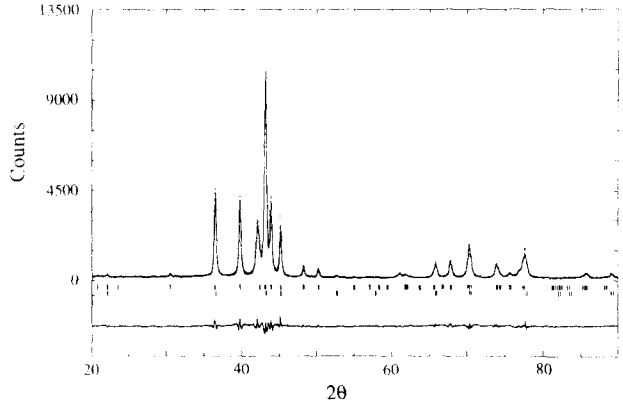

Fig. 1. Observed, calculated and difference X-ray diffraction patterns for $Zr_{0.5}Ti_{0.5}Ni_{1.3}Mn_{0.5}V_{0.2}$. Upper and lower tick marks are Bragg reflections for the C14 and C15 phases.

where S_i, D_i and V_i were the scale factor, theoretical density and volume of the ith phase respectively. $Zr_{0.5}Ti_{0.5}Ni_{1.3}Mn_{0.5}V_{0.2}$ was a mixture of the C14 phase (54 wt.%), C15 phase (34 wt.%) and BCC phase (12 wt.%). The abundance of the BCC phase was found to be less than 12 wt.% in the alloys in which C14 Laves phase was predominant ($Zr_{0.5}Ti_{0.5}Ni_{1.3}V_{0.7}$: 6 wt.%, $Zr_{0.5}Ti_{0.5}Ni_{1.3}Mn_{0.3}V_{0.4}$: 6 wt.%, $Zr_{0.5}Ti_{0.5}Ni_{1.3}Mn_{0.5}V_{0.2}$: 12 wt.%, $Zr_{0.8}Ti_{0.2}Ni_{1.3}Mn_{0.3}V_{0.4}$: 7 wt.%). The abundance of the BCC phase in alloys that were predominantly C15 Laves phase was not calculated because of the existence of a small amount of unknown phase whose small peaks appear at 38.0 and 39.3° (2θ). However, it was estimated by comparison of the diffraction patterns that the abundance of the BCC phase was less than 5%. Table 1 lists the phase analysis, phase abundance and lattice parameters of all the alloys.

$ZrMn_2$ was the prototype of the C14 Laves phase, but the $ZrNi_2$ intermetallic phase did not exist in the Zr–Ni binary system [17]. The phase analysis revealed that $ZrNi_{1.3}Mn_{0.7}$ had the C15 phase. By the substitution of Ni in the Mn site, the crystal structure changed from $MgZn_2$-type to $MgCu_2$-type structure. Interestingly the substitution allowed us to synthesize a different kind of Laves phase alloy. The major phase of the $ZrNi_{1.3}Mn_{0.7-y}V_y$ alloys ($y=0$, 0.1, 0.2, 0.4) and the $Zr_{1-x}Ti_xNi_{1.3}Mn_{0.7}$ alloys ($x=0$, 0.1, 0.2) was the C15 phase. These alloys did not contain the C14 phase. The C14 Laves phase appeared at $y=0.4$ in the $Zr_{0.8}Ti_{0.2}Ni_{1.3}Mn_{0.7-y}V_y$ alloys ($y=0$, 0.2, 0.4). In the case of $Zr_{1-x}Ti_xNi_{1.3}Mn_{0.3}V_{0.4}$, they were the pure C15 phase at $x=0$, the mixture of C14 and C15 phases at $x=0.2$. Then the C15 phase disappeared at $x=0.5$. From the above result, the C14 phase was not formed by the mono-substitution on $ZrNi_{1.3}Mn_{0.7}$ containing the C15 phase. It was necessary to perform simultaneous substitution for the formation of the C14 phase.

Fig. 2 shows the result of lattice parameters of the $Zr_{1-x}Ti_xNi_{1.3}Mn_{0.7}$ alloys ($x=0$, 0.1, 0.2) and $ZrNi_{1.3}Mn_{0.7-y}V_y$ alloys ($y=0$, 0.1, 0.2, 0.4). The lattice parameters of the $Zr_{1-x}Ti_xNi_{1.3}Mn_{0.7}$ alloys linearly decreased with increasing Ti content. In the case of the $ZrNi_{1.3}Mn_{0.7-y}V_y$ alloys, it linearly increased with increasing V content. The change of the lattice parameter by the substitution of Ti (0.0017 (1) nm/0.1 mol of Ti) was about twice as much as that by substitution of V (0.0009 (1) nm/0.1 mol of V). Therefore simultaneous substitution can more minutely control the lattice parameters compared with mono-substitution. For example, the $Zr_{0.8}Ti_{0.2}Ni_{1.3}Mn_{0.6}V_{0.1}$ and $Zr_{0.8}Ti_{0.2}Ni_{1.3}Mn_{0.5}V_{0.2}$ alloys were prepared by the substitution of 0.1 mol of Ti on the Zr site and of 0.1 and 0.2 mol of V on the Mn site of the $Zr_{0.9}Ti_{0.1}Ni_{1.3}Mn_{0.7}$. Their lattice parameters were smaller than that of the $Zr_{0.9}Ti_{0.1}Ni_{1.3}Mn_{0.7}$, and larger than that of the $Zr_{0.8}Ti_{0.2}Ni_{1.3}Mn_{0.7}$ which was substituted by 0.1 mol of Ti on Zr site of the $Zr_{0.9}Ti_{0.1}Ni_{1.3}Mn_{0.7}$.

From the above results, the change of the lattice parameters was attributed to the difference between the atomic radius of the host elements ($r_{(h.e.)}$) and that of the substituting elements ($r_{s.e.}$). When $r_{h.e.}$ is larger than $r_{s.e.}$ ($r_{h.e.} > r_{s.e.}$: Zr = 0.161 nm [18], Ti = 0.147 nm [18]), the lattice parameter decreased. Conversely, when $r_{s.e.}$ was larger than $r_{h.e.}$ ($r_{h.e.} < r_{s.e.}$: Mn = 0.112 nm [18], V = 0.137 nm [18]), the lattice parameter increased.

3.2. Pressure-composition (PC) isotherm

The PC isotherms at 313 K were measured in order to study the effect of the substitution of Ti on the Zr

Table 1
The results of X-ray diffraction measurements

Composition	Phase (wt.%)	Lattice parameters of Laves phase (nm)
$Zr_{0.5}Ti_{0.5}Ni_{1.3}V_{0.7}$	C14 (94%), BCC (6%)	$a=0.49497(5)$, $c=0.80720(6)$
$Zr_{0.5}Ti_{0.5}Ni_{1.3}Mn_{0.3}V_{0.4}$	C14 (94%), BCC (6%)	$a=0.49287(5)$, $c=0.80310(7)$
$Zr_{0.5}Ti_{0.5}Ni_{1.3}Mn_{0.5}V_{0.2}$	C14 (54%), C15 (34%), BCC (12%)	C14: $a=0.49257(5)$, $c=0.80174(6)$ C15: $a=0.69429(4)$
$Zr_{0.8}Ti_{0.2}Ni_{1.3}Mn_{0.3}V_{0.4}$	C14 (22%), C15 (71%), BCC (7%)	C14: $a=0.4990(1)$, $c=0.8128(2)$ C15: $a=0.70375(5)$
$Zr_{0.8}Ti_{0.2}Ni_{1.3}Mn_{0.5}V_{0.2}$	C15 (≈)	$a=0.70191(3)$
$Zr_{0.8}Ti_{0.2}Ni_{1.3}Mn_{0.6}V_{0.1}$	C15 (≈)	$a=0.70162(3)$
$Zr_{0.8}Ti_{0.2}Ni_{1.3}Mn_{0.7}$	C15 (≈)	$a=0.70032(3)$
$ZrNi_{1.3}Mn_{0.3}V_{0.4}$	C15 (≈)	$a=0.70709(5)$
$ZrNi_{1.3}Mn_{0.5}V_{0.2}$	C15 (≈)	$a=0.70544(4)$
$ZrNi_{1.3}Mn_{0.6}V_{0.1}$	C15 (≈)	$a=0.70443(5)$
$ZrNi_{1.3}Mn_{0.7}$	C15 (≈)	$a=0.70374(4)$
$Zr_{0.9}Ti_{0.1}Ni_{1.3}Mn_{0.7}$	C15 (≈)	$a=0.70227(3)$

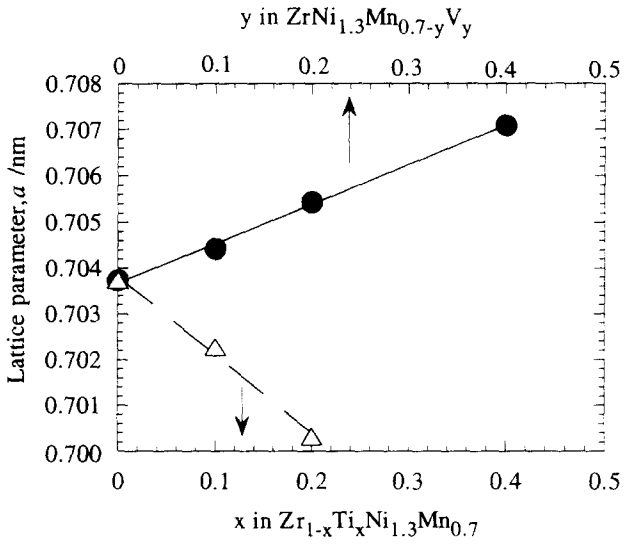

Fig. 2. The lattice parameters of the C15 phase with variation of V and Ti content. ●, $ZrNi_{1.3}Mn_{0.7-y}V_y$; △, $Zr_{1-x}Ti_xNi_{1.3}Mn_{0.7}$

Table 2
The results of PC isotherm measurements

Composition	Plateau pressure at 313 K (MPa)	Hydrogen capacity (H/M at 4 MPa)
$Zr_{0.5}Ti_{0.5}Ni_{1.3}V_{0.7}$	–	1.00
$Zr_{0.5}Ti_{0.5}Ni_{1.3}Mn_{0.3}V_{0.4}$	–	0.92
$Zr_{0.5}Ti_{0.5}Ni_{1.3}Mn_{0.5}V_{0.2}$	–	0.80
$Zr_{0.8}Ti_{0.2}Ni_{1.3}Mn_{0.3}V_{0.4}$	–	1.04
$Zr_{0.8}Ti_{0.2}Ni_{1.3}Mn_{0.5}V_{0.2}$	0.32 (0.31) [a]	1.04
$Zr_{0.8}Ti_{0.2}Ni_{1.3}Mn_{0.6}V_{0.1}$	0.58 (0.42)	0.97
$Zr_{0.8}Ti_{0.2}Ni_{1.3}Mn_{0.7}$	1.91 (0.79)	0.95
$ZrNi_{1.3}Mn_{0.3}V_{0.4}$	–	1.06
$ZrNi_{1.3}Mn_{0.5}V_{0.2}$	0.15 (0.12)	1.11
$ZrNi_{1.3}Mn_{0.6}V_{0.1}$	0.57 (0.21)	1.04
$ZrNi_{1.3}Mn_{0.7}$	1.59 (0.33)	0.89
$Zr_{0.9}Ti_{0.1}Ni_{1.3}Mn_{0.7}$	1.53 (0.48)	1.02

[a] Hydrogen equilibrium plateau pressure of desorption is given in parentheses.

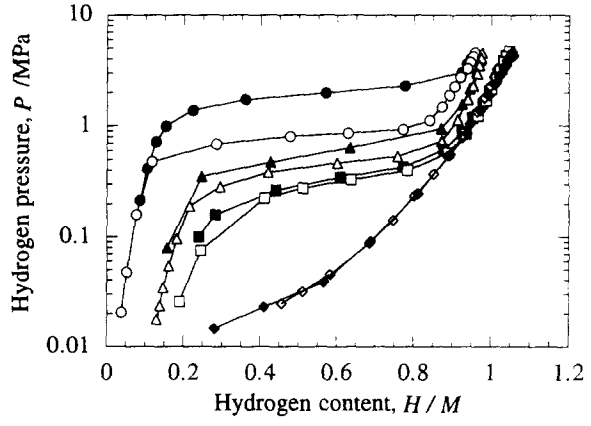

Fig. 3. Pressure-composition isotherms for $Zr_{0.8}Ti_{0.2}Ni_{1.3}Mn_{0.7-y}V_y$ at 313 K. $Zr_{0.8}Ti_{0.2}Ni_{1.3}Mn_{0.7}$, ● (absorb), ○ (desorb); $Zr_{0.8}Ti_{0.2}Ni_{1.3}Mn_{0.6}V_{0.1}$, ▲ (absorb), △ (desorb); $Zr_{0.8}Ti_{0.2}Ni_{1.3}Mn_{0.5}V_{0.2}$, ■ (absorb), □ (desorb); $Zr_{0.8}Ti_{0.2}Ni_{1.3}Mn_{0.3}V_{0.4}$, ◆ (absorb), ◇ (desorb).

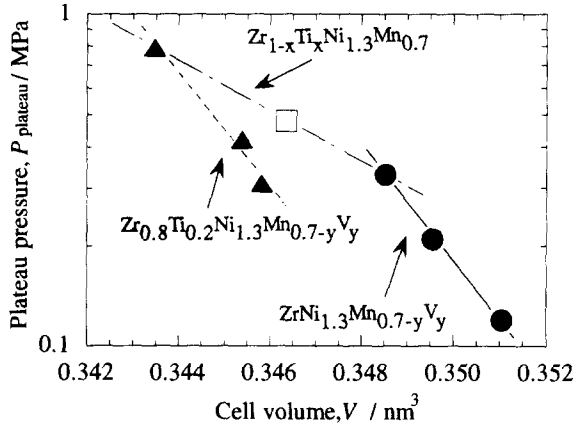

Fig. 4. Relation between the cell volume and plateau pressure of desorption at 313 K for $Zr_{0.8}Ti_{0.2}Ni_{1.3}Mn_{0.7-y}V_y$ (– – –), $ZrNi_{1.3}Mn_{0.7-y}V_y$ (——) and $Zr_{1-x}Ti_xNi_{1.3}Mn_{0.7}$ (– · –).

(A) site and of V on the Mn (B) site on the hydrogen absorbing-desorbing properties (hydrogen equilibrium plateau pressure, hydrogen absorbing capacity and hysteresis). Fig. 3 shows the typical PC isotherms of the hydrogen absorption-desorption for the $Zr_{0.8}Ti_{0.2}Ni_{1.3}Mn_{0.7-y}V_y$ ($y = 0, 0.1, 0.2, 0.4$) alloys. Hydrogen content was denoted as the ratio of hydrogen to metal, H/M. All the alloys were found to reversibly react with a large amount of hydrogen ($0.8 \leqslant H/M \leqslant 1.11$) at 313 K. Clear plateaus were observed in the isotherms of the alloys whose major phase was the C15 phase as shown in Fig. 3. The hydrogen equilibrium plateau pressures (so called plateau pressure) of both absorption and desorption were defined as the equilibrium pressure at the center of the plateau region. Table 2 lists the plateau pressures obtained from the isotherms. The maximum hydrogen absorbing capacity (so called hydrogen capacity) of each alloy was the value of the H/M ratio under the equilibrium pressure of 4 MPa at 313 K, listed in Table 2. The PC isotherm results showed that an increase of V (B-site) content resulted in the lowering of the plateau pressure, and that the plateau pressures increased with increasing Ti (A-site) content.

It was reported that the plateau pressure has a linear relationship against the cell volume of the alloys. This relationship was found in the rare earth–nickel based AB_5 alloy [19] and Zr based AB_2 alloys [1]. The logarithm of the plateau pressure ($\ln(P_{plateau}/MPa)$) was represented as a function of the cell volume of the alloys in Fig. 4. The $\ln P_{plateau}$ of the $ZrNi_{1.3}Mn_{0.7-y}V_y$ alloys ($y = 0$, 0.1, 0.2) linearly decreased with increasing cell volume (-178 (8) nm^{-3}). This correlation was observed when the composition of either A or B sites was held constant, for example the $Zr_{1-x}Ti_xNi_{1.3}Mn_{0.7}$ alloys ($x = 0$,

0.1, 0.2) and $Zr_{0.8}Ti_{0.2}Ni_{1.3}Mn_{0.7-y}V_y$ alloys ($y=0$, 0.1, 0.2). The slope of $\ln P_{plateau}$ against the cell volume of the $ZrNi_{1.3}Mn_{0.7-y}V_y$ alloys was almost identical to that of the $Zr_{0.8}Ti_{0.2}Ni_{1.3}Mn_{0.7-y}V_y$ alloys (-163 (23) nm^{-3}), and larger than that of the $Zr_{1-x}Ti_xNi_{1.3}Mn_{0.7}$ alloys (-75.0 (2) nm^{-3}). We took into account the relationship between lattice parameters and the content of the replacing elements discussed in Section 3.1. The change of the plateau pressure by substituting V was larger than that by substituting Ti. Simultaneous substitution can control more minutely the plateau pressure compared with mono-substitution. For example, the substitution of 0.2 mol of Ti in the Zr site of the $ZrNi_{1.3}Mn_{0.7}$ results in an increase of the plateau pressure from 0.33 to 0.79 MPa (desorption). On the other hand, the $Zr_{0.8}Ti_{0.2}Ni_{1.3}Mn_{0.6}V_{0.1}$ alloy was synthesized by the substitution of 0.2 mol of Ti in the Zr site and of 0.1 mol of V in the Mn site of the $ZrNi_{1.3}Mn_{0.7}$. Its plateau pressure was 0.42 MPa, which was between that of $ZrNi_{1.3}Mn_{0.7}$ and $Zr_{0.8}Ti_{0.2}Ni_{1.3}Mn_{0.7}$.

We suggested in Section 3.1 that the lattice-expansion and contraction by the substitution was predicted from the $r_{s.e.}/r_{h.e.}$ ratio. It was discussed there that the plateau pressure closely correlated with the cell volume. Accordingly, the $r_{s.e.}/r_{h.e.}$ ratio was presumably a good index to predict whether or not the plateau pressure of the modified alloy became higher or lower depending on the volume of the modified alloy.

The hydrogen capacity is an important piece of information to evaluate the hydrogen absorbing alloys. The hydrogen capacity directly influenced the performance of each application, but it cannot be predicted from the physical properties of the alloy. in addition, hydrogen capacity was an arbitrary value depending on the H/M ratio at a given equilibrium pressure and temperature on the PC isotherm. Therefore it was important to set the pressure, P_{max}, at which the H/M ratio was defined as the hydrogen capacity. Fig. 5 schematically shows how to define the hydrogen capacity. We assume the presence of two alloys as follows: (1) alloys A and B have isotherms of the same shape, (2) but their plateau pressures are different. We define the hydrogen capacity at P_{max}. When the plateau pressure of the alloy B is lower than that of the alloy A, the hydrogen capacity of alloy B is automatically larger than that of alloy A. When we define the hydrogen capacity at P'_{max}, the characteristics become completely different. The shape of the isotherms, however, is not always identical. That is one of the reasons we found some discrepancies in the relation between the plateau pressure and hydrogen capacity. The hydrogen capacities were found to depend on the plateau pressure in the cases of $Zr_{0.8}Ti_{0.2}Ni_{1.3}Mn_{0.7-y}V_y$ ($y=0$, 0.1 0.2, 0.4) and $ZrNi_{1.3}Mn_{0.7-y}V_y$ ($y=0$, 0.1, 0.2). There is one exceptional case in the $Zr_{1-x}Ti_xNi_{1.3}Mn_{0.7}$ alloys. The plateau pressure decreases in the order $Zr_{0.8}Ti_{0.2}Ni_{1.3}Mn_{0.7} > Zr_{0.9}Ti_{0.1}Ni_{1.3}Mn_{0.7} > ZrNi_{1.3}Mn_{0.7}$. However, the hydrogen capacity increases as $Zr_{0.9}Ti_{0.1}Ni_{1.3}Mn_{0.7} > Zr_{0.8}Ti_{0.2}Ni_{1.3}Mn_{0.7} > ZrNi_{1.3}Mn_{0.7}$.

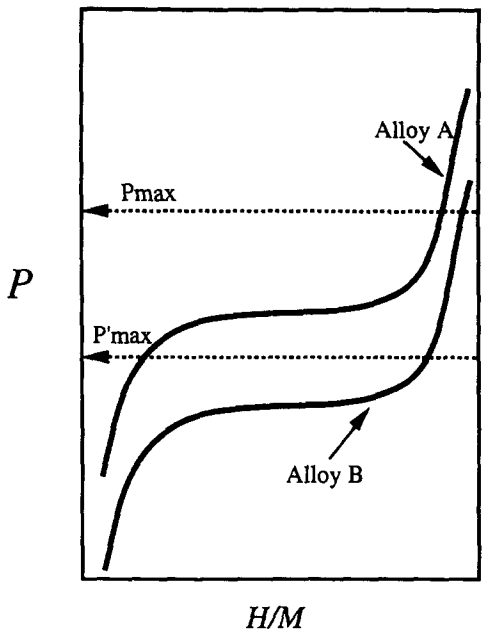

Fig. 5. Schematic drawing of the relationship between plateau pressure and the hydrogen capacity.

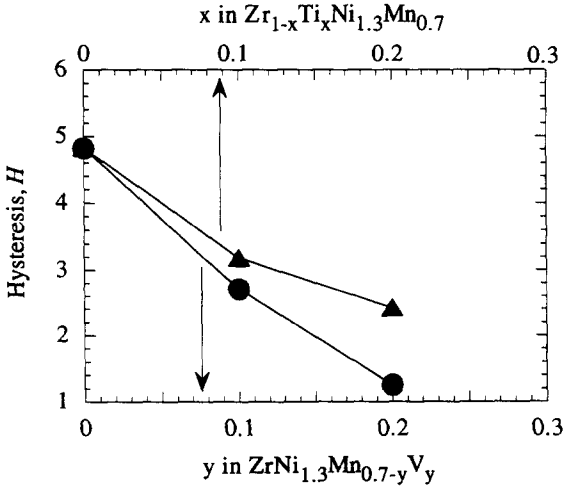

Fig. 6. Variation of hysteresis (P_{absorb}/P_{desorb}) with V and Ti content in the PC isotherms for the C15 phase alloys.

From the above results and discussion, the plateau pressure was found to correlate to the hydrogen capacity. Generally, lowering the plateau pressure tends to increase the hydrogen capacity. It is clear that substitution of V on the Mn site effectively increases the hydrogen capacity. Therefore, if we adopt the replacing elements for the Zr and Mn sites that have the effect of decreasing the plateau pressure, namely the $r_{s.e.}/r_{h.e.}$ ratios are more than one, an alloy with much higher hydrogen capacity results.

We did not observe significant differences in the hydrogen absorbing capacity between the C14 and C15

phases (Table 2). The PC isotherms of multiphase alloys ($Zr_{0.5}Ti_{0.5}Ni_{1.3}Mn_{0.5}V_{0.2}$ and $Zr_{0.8}Ti_{0.2}Ni_{1.3}Mn_{0.3}V_{0.4}$) did not show any discontinuous change caused by the existence of more than one phase. Remarkably the multiphase alloys behave as a single phase alloy in the PC isotherms.

A large hysteresis was observed in the PC isotherm of $Zr_{0.8}Ti_{0.2}Ni_{1.3}Mn_{0.7}$ alloy. The magnitude of hysteresis was represented as the ratio of the plateau pressure of absorption and desorption, P_{absorb}/P_{desorb} (H) as shown in Fig. 6. This hysteresis was reduced with the increase of Ti content in the $Zr_{1-x}Ti_xNi_{1.3}Mn_{0.7}$ alloys ($x=0$, 0.1, 0.2) and with increase of V content in the $ZrNi_{1.3}Mn_{0.7-y}V_y$ alloys ($y=0$, 0.1, 0.2). The simultaneous substitution of Ti and V is more effective for the decrease of hysteresis than the mono-substitution. For example, the ratio H of $Zr_{0.8}Ti_{0.2}Ni_{1.3}Mn_{0.5}V_{0.2}$ ($H=1.03$) is smaller than that of $ZrNi_{1.3}Mn_{0.5}V_{0.2}$ ($H=1.25$) (Table 2) when compared with that of $ZrNi_{1.3}Mn_{0.7}$.

4. Conclusion

We studied the effect of the substitutions of Ti on the Zr (A) site and of V on the Mn (B) site of the $ZrNi_{1.3}Mn_{0.7}$ alloy on the phase stability, lattice parameters, plateau pressure and hysteresis.

(1) There exist three phases; the C14, C15 phases and the BCC solid solution phase in twelve alloys studied. The C14 phase forms only by the simultaneous substitution of Ti on the Zr site and V on the Mn site of the $ZrNi_{1.3}Mn_{0.7}$ containing C15 phase.

(2) The increase of Ti content on the A site results in the decrease of the lattice parameter and the increase of the plateau pressure; in contrast, the increase of V content on the B site leads to an increase of the lattice parameter and the lowering of the plateau pressure. The simultaneous substitution can more minutely control the lattice parameter and plateau pressure in comparison with mono-substitution.

(3) The unit cell volume of a given alloy linearly decreases with increase of the logarithm of the plateau pressure while compositions containing either A or B site substitutions remain constant. The hydrogen capacity increases with decreasing plateau pressure.

(4) The simultaneous substitution is more effective for decreasing the hysteresis than mono-substitution.

Acknowledgments

We thank Mr. Y. Ishido of Shin-Kobe Electric Machinery Co., Ltd. and Mr. K. Nomura of the National Institute of Materials and Chemical Research for technical assistance, and Dr. B. Baldwin of the National Institute of Materials and Chemical Research for editorial comments.

References

[1] S. Fujitani, I. Yonezu, T. Saito, N. Furukawa, E. Akiba, H. Hayakawa and S. Ono, *J. Less-Common Met., 172–174* (1991) 220.
[2] T. Sakai, K. Oguro, H. Miyamura, N. Kuriyama, A. Kato, H. Ishikawa and C. Iwakura, *J. Less-Common Met., 161* (1990) 193.
[3] S. Wakao and H. Sawa, *Denki Kagaku, 59* (1991) 950.
[4] F. Laves and H. Witte, *Metalluwirtsschft, 15* (1936) 840.
[5] P. Villars and L.D. Calvert, *Pearson's Handbook of Crystallographic Data for Intermetallic Phases*, Vol. 4, ASM International, Materials Park, 1993, p. 4406.
[6] P. Villars and L.D. Calvert, *Pearson's Handbook of Crystallographic Data for Intermetallic Phases*, Vol. 4, ASM International, Materials Park, 1993, p. 5354.
[7] I. Yonezu, S. Fujitani, A. Furukawa, K. Nasako, T. Yonesaki, T. Saito and N. Furukawa, *J. Less-Common Met., 168* (1991) 201.
[8] E. Akiba, H. Hayakawa, S. Fujitani, I. Yonezu, D. Fruchart, J.L. Soubeyroux, L. Pontonnier and S. Miraglia, *Proc. 5th Int. Symp. Adv. Nuclear Energy Res.*, JAERI, 1993, p. 300.
[9] J.-J. Didisheim, K. Yvon, D. Shaltiel and P. Fischer, *Solid State Commun., 31* (1979) 47.
[10] F. Pourarian, V.K. Sinha, W.E. Wallace and H.K. Smith, *J. Less-Common Met., 88* (1982) 451.
[11] A. Suzuki, N. Nishimiya, *Mat. Res. Bull., 19* (1984) 1559.
[12] P. Villars and L.D. Calvert, *Pearson's Handbook of Crystallographic Data for Intermetallic Phases*, Vol. 3, ASM International, Materials Park, 1993, p. 2754.
[13] F. Izumi, in R.A. Young (ed.), *The Rietveld Method*, Oxford University Press, Oxford, 1993, Ch. 13.
[14] K. Nomura, H. Uruno, S. Ono, H. Shinozuka and S. Suda, *J. Less-Common Met., 107* (1985) 221.
[15] J. Huot, E. Akiba, T. Ogura and Y. Ishido, *Denki Kagaku, 61* (1993) .
[16] R.J. Hill, *Powder Diffraction, 6* (1991) 74.
[17] W.G. Moffatt, *The Handbook of Binary Phase Diagrams*, Genium Publishing Corporation, New York, 1984.
[18] E.A. Brandes and G.B. Brook, *Smithells Metal Reference Book*, Butterworth-Heinemann, Oxford, 1992.
[19] M.H. Mendelsohn, D.M. Gruen and A.E. Dwight, *Nature, 269*, (1977) 45.